Column Integrated Aerosol Properties During the May 2003 Aerosol IOP

P. Ricchiazzi and C. Gautier
Institute for Computational Earth System Science (ICESS)
University of California
Santa Barbara, California

Background

Some recent studies of clear-sky radiation indicate that current radiative transfer (RT) models tend to underestimate atmospheric absorption when the aerosol optical depth is small and standard aerosol properties are assumed. This so-called clear-sky anomaly is manifested in predicted levels of diffuse radiation significantly above those observed at Southern Great Plains (SGP) and other sites in the continental U.S. (e.g., Halthore et al. 1998 GRL). In general, observations made at pristine sites do not show a discrepancy (Barnard and Powell 2001: [North Slope Alaska] 2001; Kato et al. 1999: [Mauna Loa]), Halthore 1998 [South Pole]). However, the anomaly did appear in observations obtained at Palmer Station, Antarctica [Payton, et al., 2002 ARM STM]). The concurrent observations made during the May 2003 aerosol intensive operational period (IOP) provide a valuable test of in-situ and ground based aerosol retrieval techniques, and allow detailed evaluation of radiative closure.

Data

- in-situ **aerosol scattering coefficient** in green channel from total sky imager (TSI) nephelometer on IAP flights
- in-situ **absorption coefficient** from Radiance Research particle/soot absorption photometer (PSAP) absorption photometer on IAP flights
- effective **surface albedo** estimated as an areal average of the measured spectral albedo of several landcover types within 10 km radius around the central facility.
- vertical **aerosol optical depth profile** from Ames Airborne Tracking Sunphotometer (AATS) Ames
- aerosol volume distribution from Cimel sunphotometer (CSPOT) aereole data (based on Nakajima et al., 1983 retrieval technique)
- **almucantor and principle plane radiance scans** from CSPOT
- **aerosol optical depth** from CSPOT
- **total and diffuse irradiance** from multi-filter rotating shadowband radiometer (MFRSR).

Method

In this study, aerosol phase function (P) and single-scattering albedo (SSA) (ω) are retrieved from CSPOT observations of sky-radiance for several days during the IOP. The retrieval method is based on the iterative technique described by Wang and Gordon (WG 1993), and uses a Monte-Carlo radiative

transfer model (Ricchiazzi and Gautier 1998) to provide accurate forward calculations of radiance in the areole region. IOP data for aerosol optical depth from the Ames airborne tracking sunphotometer (AATS) and IAP flights (Figures 1 and 2) were used in the radiative transfer calculations. The first quantity produced by the iterative procedure is the product of the SSA and the scattering phase function, sampled at all viewing azimuth and zenith angles accessible to the CSPOT either on the principal plane or around an almucantor scan. In the WG method the phase function is assumed constant over the small range of scattering angles that can not be directly observed by the sun photometer (e.g., near the backward scattering direction). Once a converged value of ωP is obtained (Figure 4), the SSA is retrieved by applying the normalization condition on the phase function, i.e.: $\omega = \frac{1}{2} \int \omega P \, d\mu$, where μ is the cosine of the scattering angle. The retrieved values of phase function divided by the Mie phase function varied between 0.7 to 1.5 on most days (Figure 5). The ratio was nearest to one for scattering angles between 30 and 45 degrees. This angular range also showed the least sensitivity to the aerosol refractive index. The Mie phase functions were computed using Mie scattering theory and the aerosol size distribution observed by CSPOT and recorded in the SGPSs photsize dataset. We compared the retrieved values of SSA (Figures 6 and 7) and backscattering fraction ($b = \int_{\mu<0} P \, d\mu / \int P \, d\mu$) (Figure 8) to in-situ values of the scattering and absorption coefficients, as observed during the IAP flights. As a final step, SBDART (Ricchiazzi et al. 1998) computations of diffuse and direct irradiance, using the retrieved phase function and SSA, were compared to MFRSR observations at the for the same time (Figures 9 and 10).

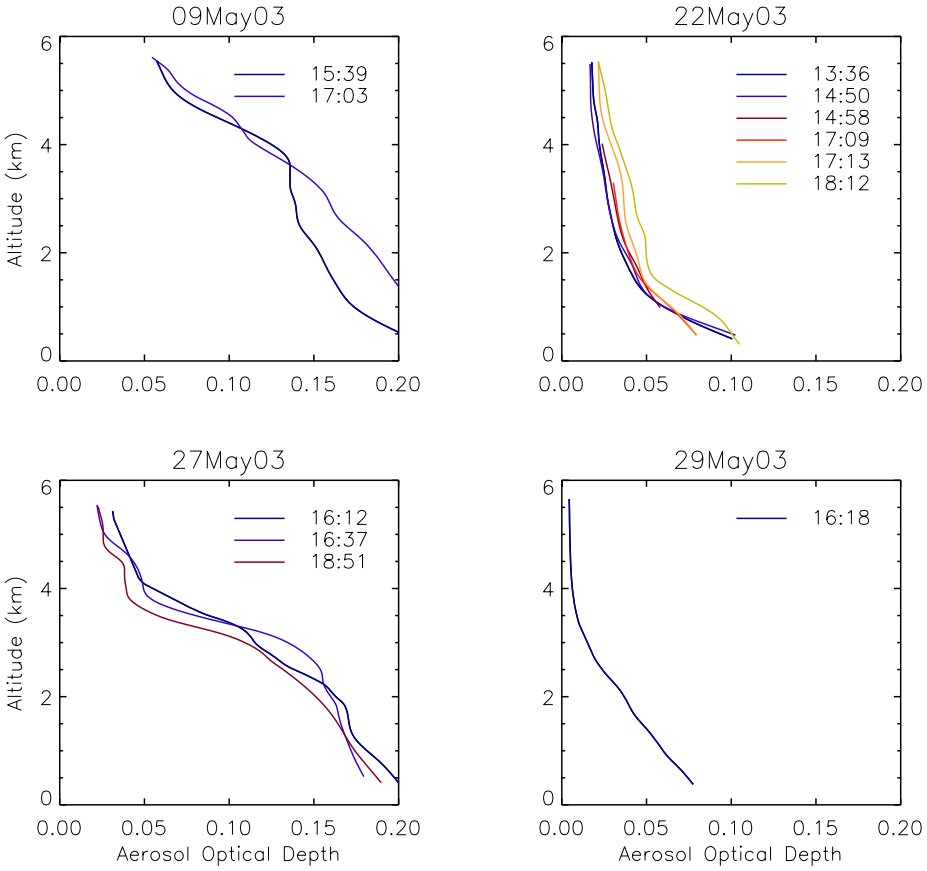

Figure 1. Aerosol optical depth profiles from AATS.

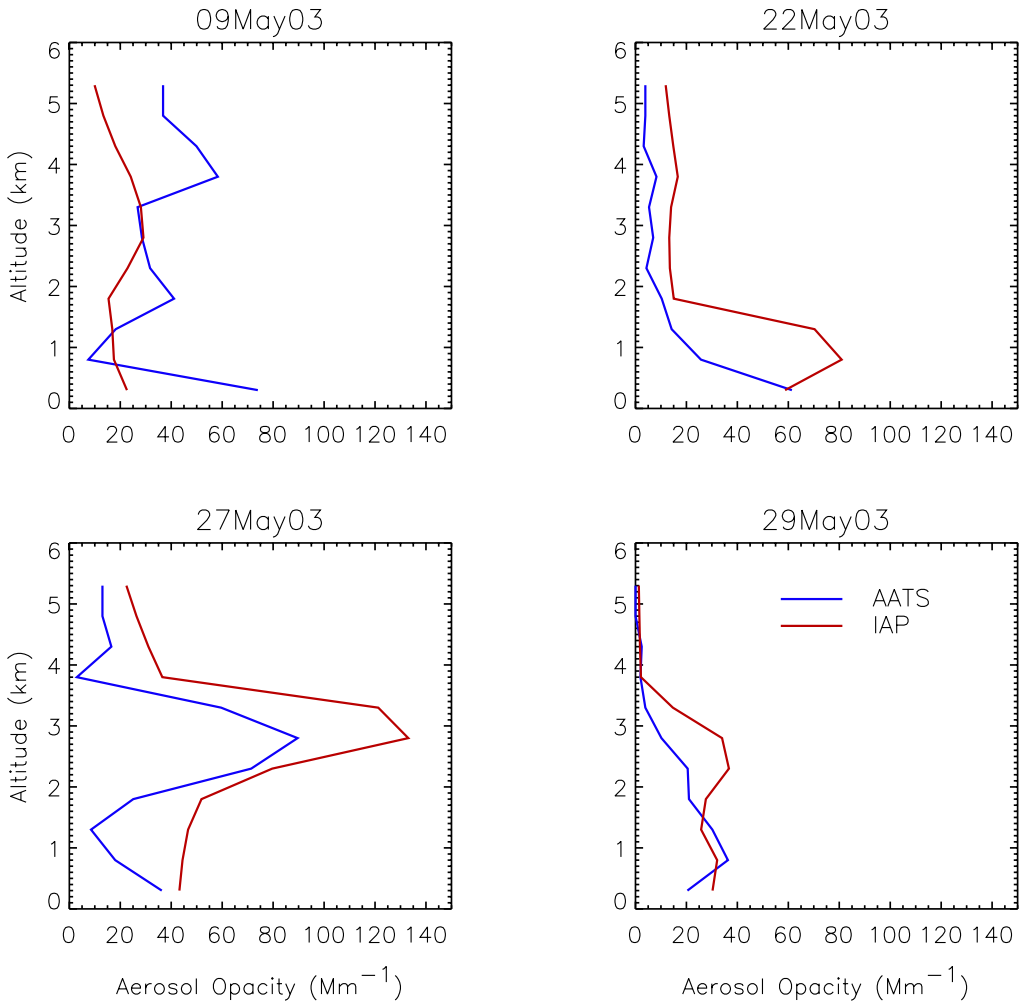

Figure 2. Profiles of extinction coefficient from IAP flights and AATS (computed from mean slope of all scans).

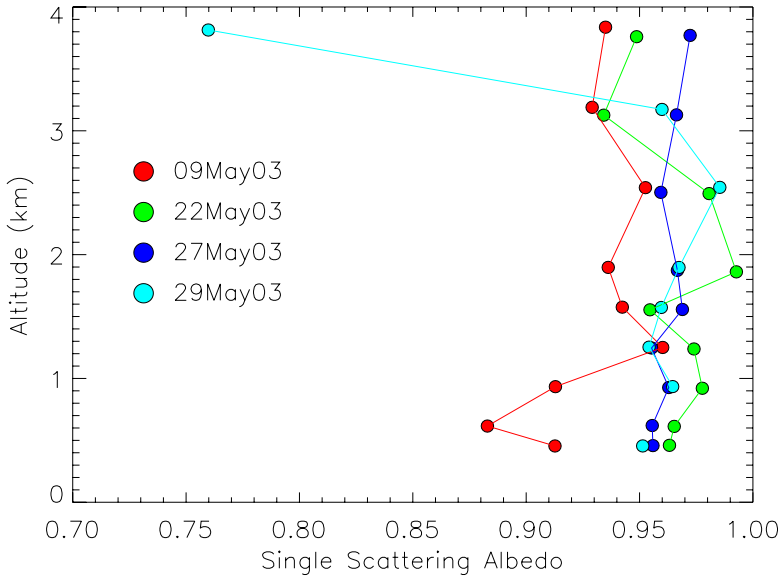

Figure 3. SSA (from scattering coefficient {green channel) and absorption coefficient).

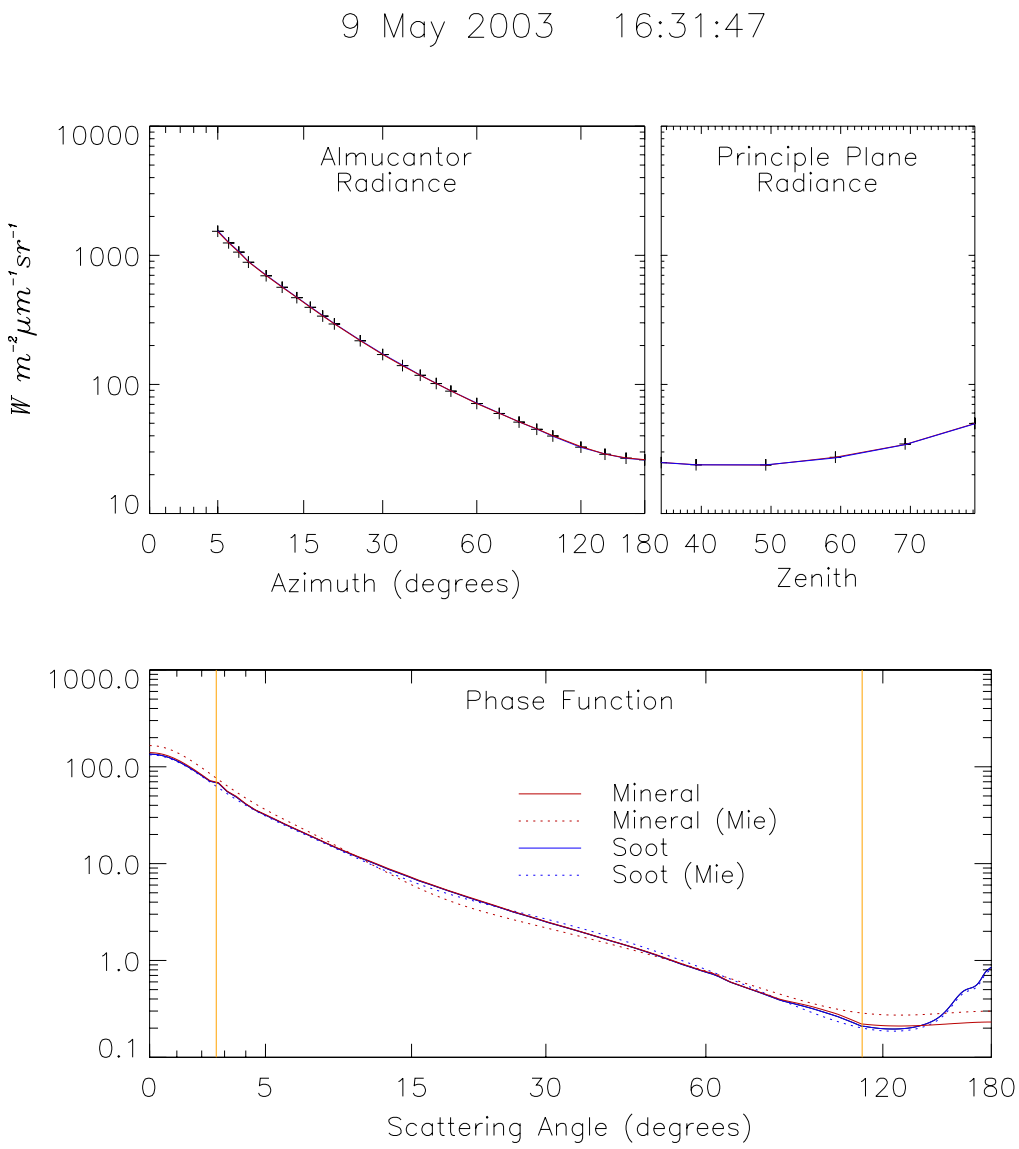

Figure 4. CSPOT radiance (676nm channel, upper) and retrieved phase function for the 9th and 29th of May. Mie scattering calculations with several assumed aerosol types were used to fill in phase function shape for scattering angles unobserved by the CSPOT radiance scans (indicated by vertical yellow lines). The results for mineral (red) and soot (blue) are shown in lower panels. The standard WG approach assumes the scattering phase function is constant throughout the range of unobserved scattering angles.

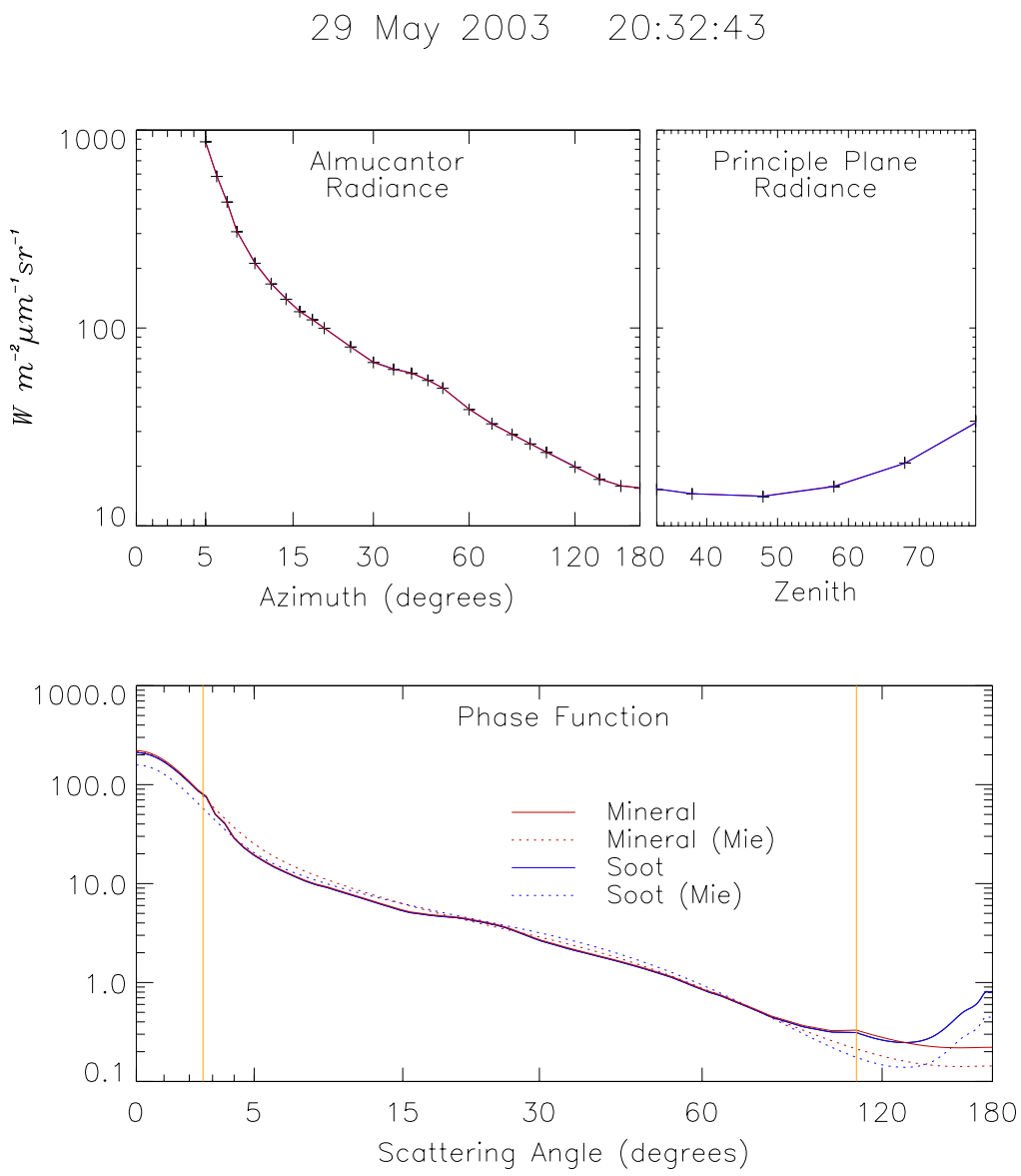

Figure 4. (contd).

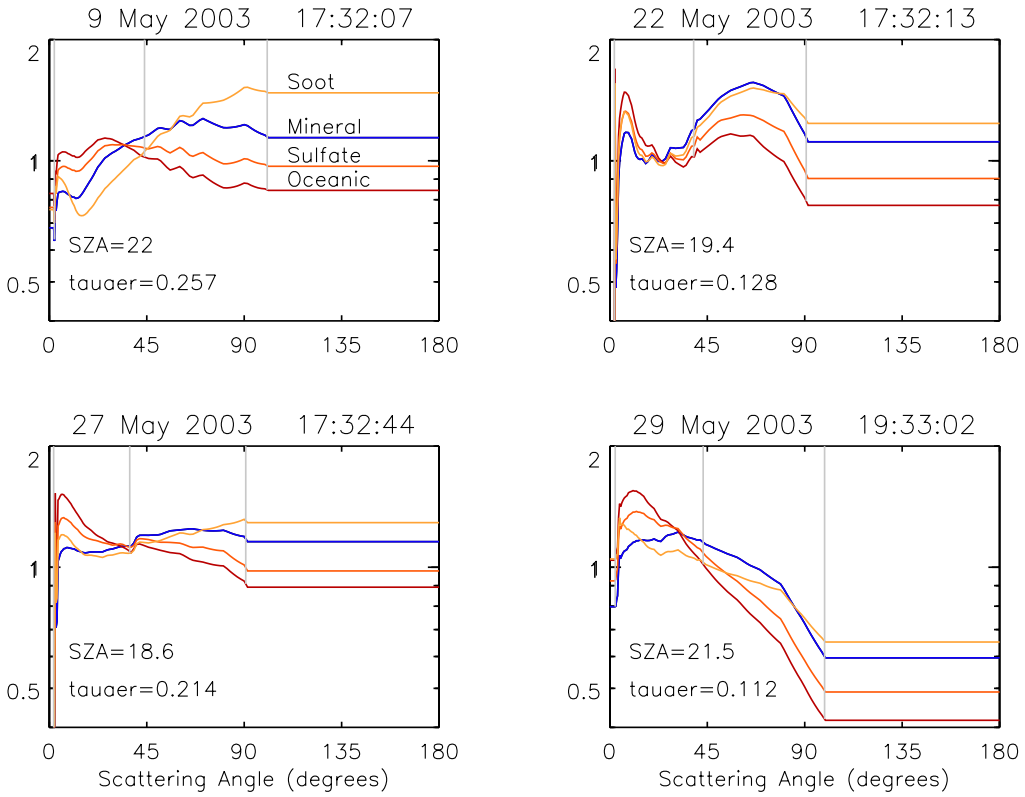

Figure 5. Ratio of Mie scattering phase function (depends on assumed aerosol type and CSPOT volume distribution) divided by retrieved phase function for selected observation times.

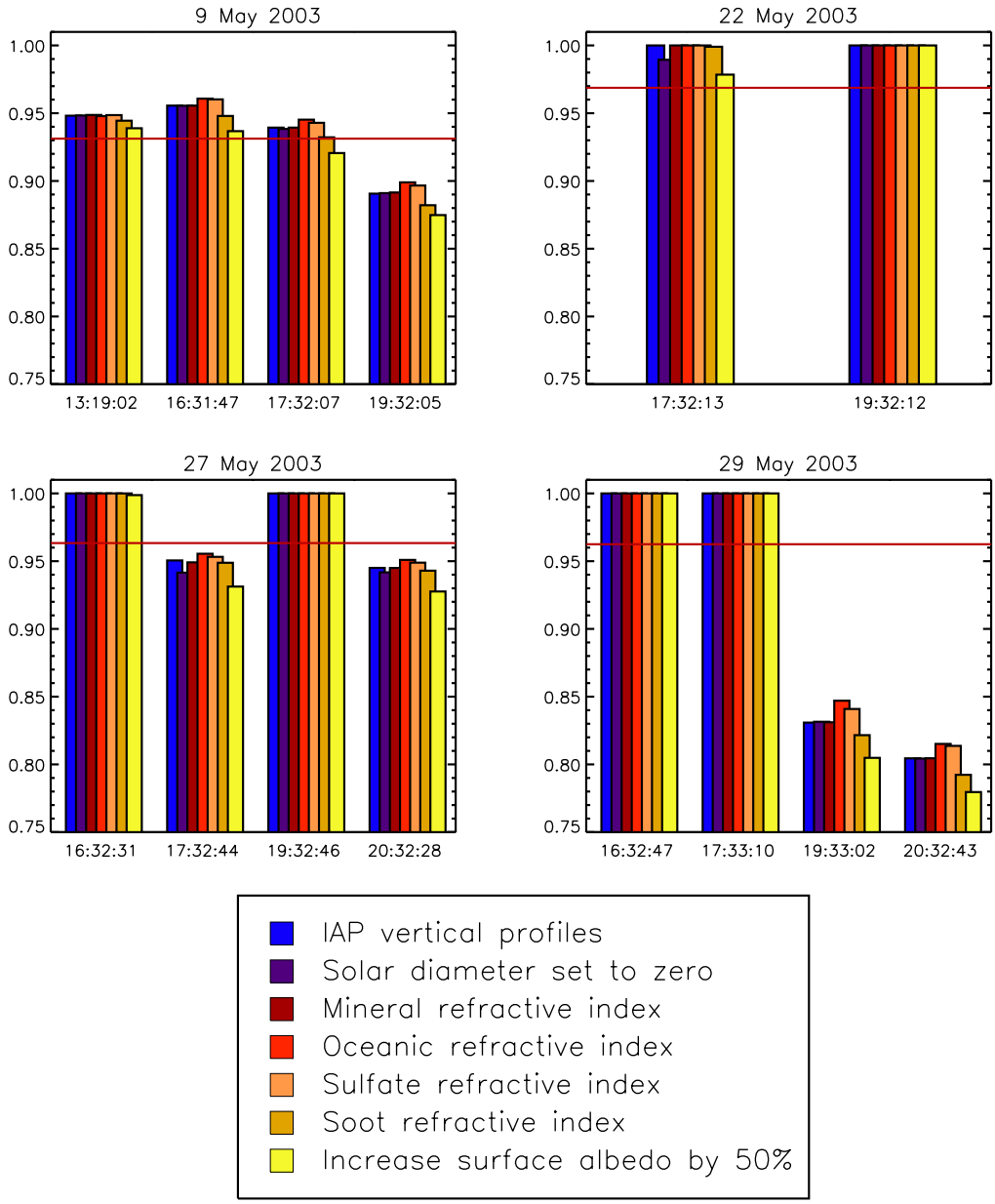

Figure 6. Aerosol SSA (obtained from $\omega = \frac{1}{2} \int \omega P \, d\mu$) compared to IAP value (solid line). The colored bars indicate different assumptions used for the phase function in the range of scattering angles unobserved by the CSPOT radiance scans. The dark blue (left-most) bar in each cluster indicates the effect of using aerosol vertical profile derived from the IAP in-situ measurements (all other cases used the AATS profiles). The yellow (right-most) bar in each cluster shows the results of increasing the surface albedo by 50% over the nominal value measured by Trischenko's group.

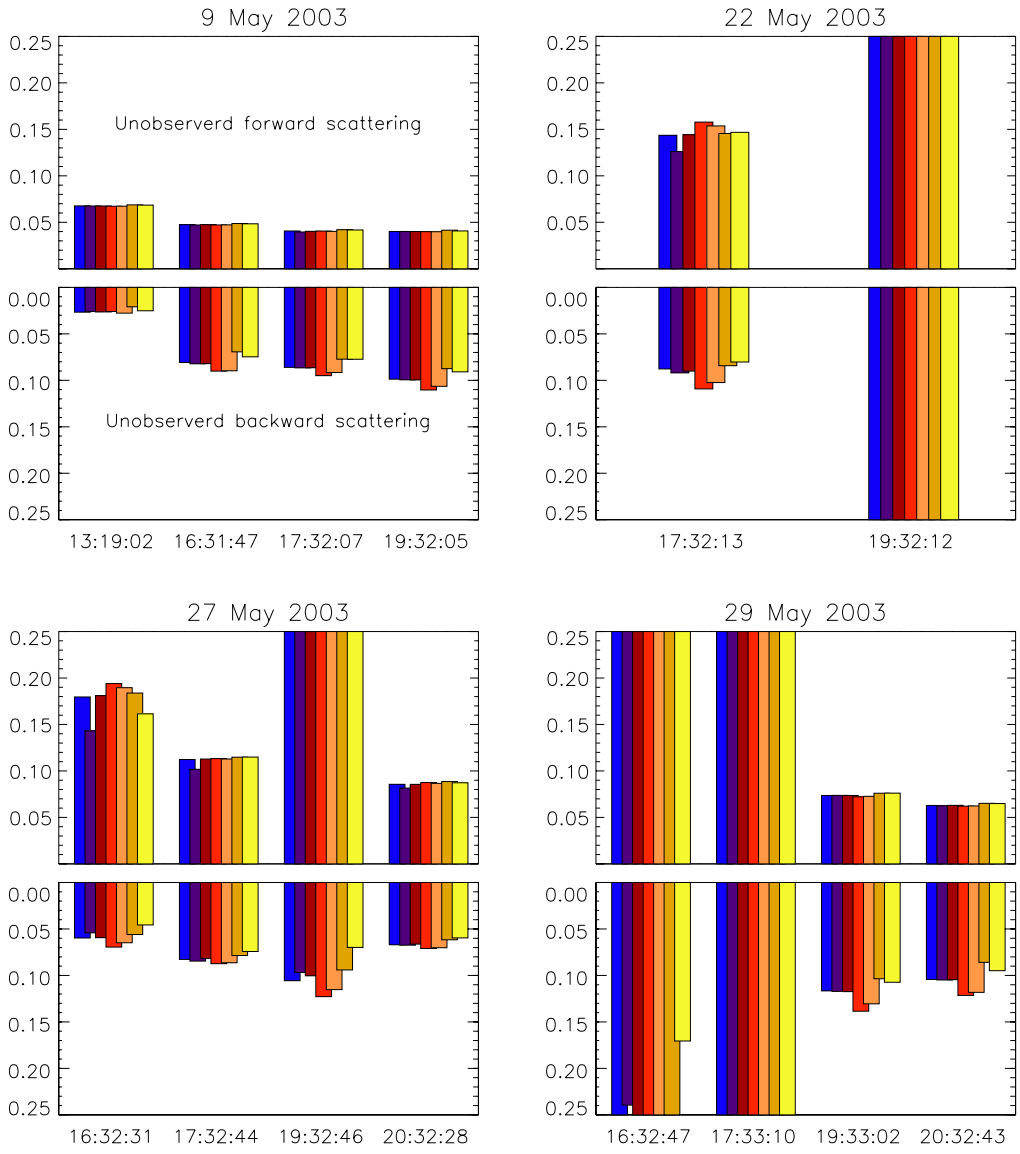

Figure 7. Aerosol SSA contributed by unobserved scattering angles.

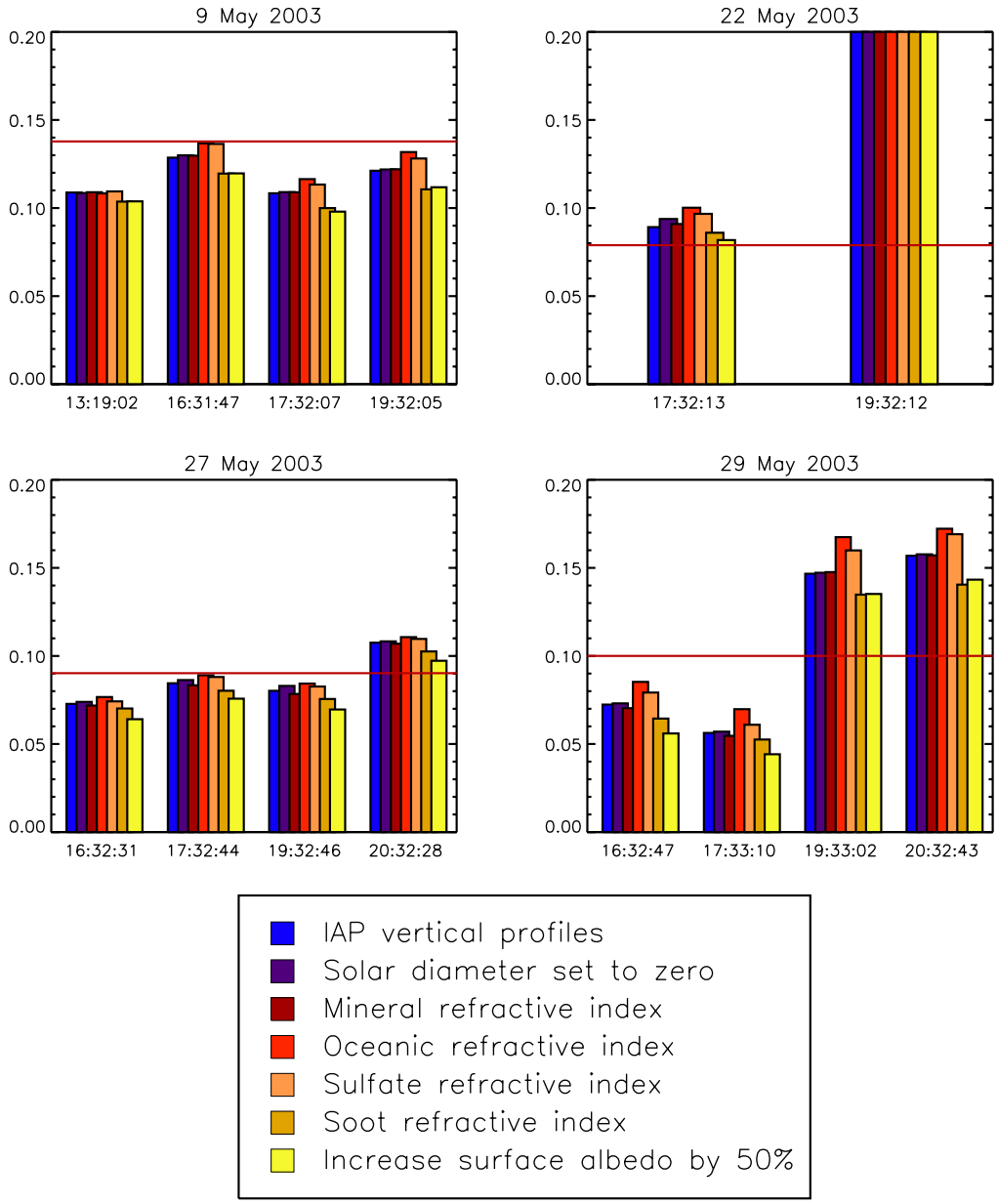

Figure 8. Retrieved backscattering ratio (*b*) compared to IAP value (horizontal solid line). $b = \int_{\mu<0} P\, d\mu / \int P\, d\mu$.

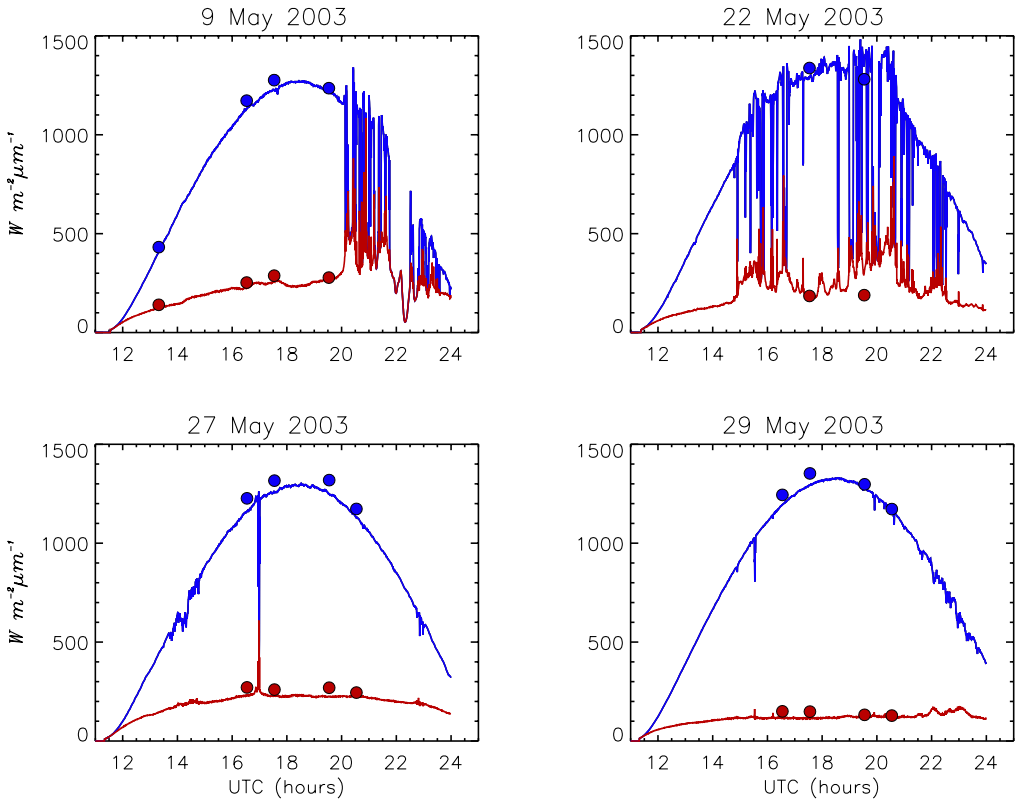

Figure 9. MFRS channel 4 (672nm) vs. total and diffuse irradiance computed by SBDART using retrieved aerosol properties.

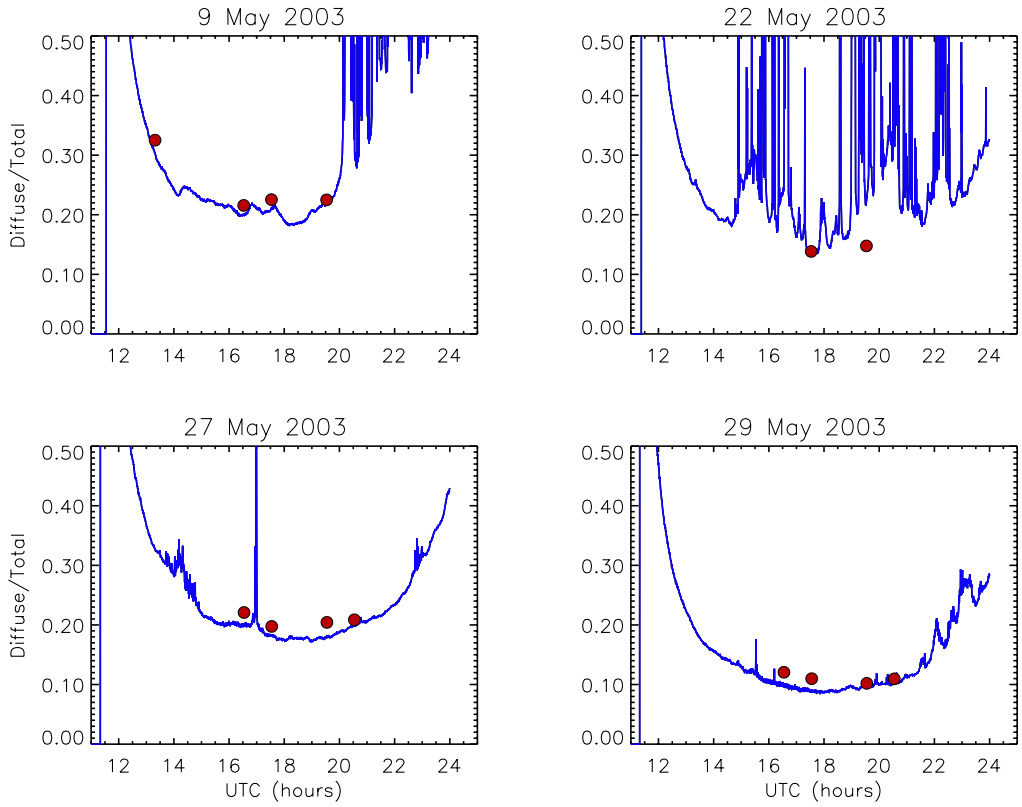

Figure 10. Ratio of MFRSR channel 4 (672nm) vs. total and diffuse irradiance computed by SBDART using retrieved aerosol properties (assuming mineral type).

Conclusions

Retrieved ω and b are close to in-situ values for most days. In cases where the agreement is poor, the problem can be traced to cloud contamination, as identified by ragged phase function profiles in the areole region. One might be tempted to explain the low value of ω on May 29 as due to an absorptive layer above IAP flight ceiling (a much smaller ω is found at the highest IAP level in Figure 3). However, AATS optical depths indicate very little extinction optical depth above that level.

On most days retrieved phase function was within 30% to 50% of the Mie scattering phase function, depending on which aerosol type was used to fill in the phase function at unobserved scattering angles.

Diffuse irradiance computed by SBDART varies between 0 to 10% larger than MFRSR observations (ignoring the cloud contaminated observations on May 22). The closest match to the MFRSR diffuse/total ratio is obtained for the retrievals of SSA at 19:32 of May 9 or at 19:33 and 20:32 of May 29. These three retrievals produced SSAs that were more than 5% smaller than the in-situ measurements (the last two May 29 retrievals were about 18% below the in-situ values). At other times a reduction in SSA of about 10% brings the SBDART results in line with the MFRSR observations.

Acknowlegments

We would like to thank the following instrument mentors for providing the observations data used in this study: Beat Schmid (AATS); John Ogren, aerosol observing system (AOS); Mark Miller (CSPOT); Donna Flynn (MFRSR); Alexander Trishchenko (surface albedo).

References

Barnard J. C. and D. M. Powell, 2002: A comparison between modeled and measured clear-sky radiative shortwave fluxes in Arctic environments, with special emphasis on diffuse radiation. *J. of Geophys. Res.-Atmos.*, **107**(D19):4383.

Halthore, R. N., S. Nemesure, S. E. Schwartz, D. G. Imre, A. Berk, E. G. Dutton, and M. H Bergin, 1998: Models overestimate diffuse clear-sky surface irradiance: A case for excess atmospheric absorption. *Geophys. Res. Lttrs*., **25**:3591-3594.

Henyey, L. G. and J. L. Greenstein, 1941: Diffuse Radiation in the Galaxy. *J. Astrophys.,* **93**:70-83.

Kato, S., T. P. Ackerman, E. G. Dutton, N. S. Laulainen, and N. Larson. "A Comparison of Modeled and Measured Irradiances for a Molecular Atmosphere." Presented at the AAAR 16th Annual Meeting, October 13-17, 1997, Denver, Colorado.

Michalsky, J. 2003: http://hog.asrc.cestm.albany.edu/~rsr

Payton, A., P.J. Ricchiazzi, and C. Gautier, 2003: Discrepancies in Shortwave Diffuse Measured and Modeled Irradiances in Antarctica. In *Proceedings of the Thirteenth Atmospheric Radiation Measurement (ARM) Science Team Meeting*, ARM-CONF-2003. U.S. Department of Energy, Washington, D.C. Available URL: http://www.arm.gov/publications/proceedings/conf13/extended_abs/francis-j.pdf

Ricchiazzi, P., S. R. Yang, C. Gautier and D. Sowle, 1998: SBDART: A research and teaching software tool for plane-parallel radiative transfer in the Earth's atmosphere. *Bulletin of the American Meteorological Society*. **79**(10):2101-2114.

Ricchiazzi, P. and C. Gautier, 1998: Investigation of the effect of surface heterogeneity and topography on the radiation environment of Palmer Station, Antarctica, with a hybrid 3-D radiative transfer model. *J. of Geophys. Res.-Atmos*. **103**(D6):6161-6176.

Wang, M. and H. Gordon, 1994: Estimating aerosol optical properties over the oceans with the multiangle imaging spectroradiometer: Some preliminary studies. *Appl. Opt.,* **33**:4042–4057.